The Journal of Infectious Diseases

MAJOR ARTICLE

The Existing Drug Vorinostat as a New Lead Against Cryptosporidiosis by Targeting the Parasite Histone Deacetylases

Fengguang Guo,[1,2] Haili Zhang,[2] Nina N. McNair,[3] Jan R. Mead,[3,4] and Guan Zhu[2]

[1]Key Laboratory for Zoonoses Research, Ministry of Education, Institute of Zoonosis, Jilin University, Changchun, China; [2]Department of Veterinary Pathobiology, College of Veterinary Medicine and Biomedical Sciences, Texas A&M University, College Station; and [3]Department of Pediatrics, Emory University, Atlanta, and [4]Atlanta Veterans Affairs Medical Center, Decatur, Georgia

Background. Cryptosporidiosis affects all human populations, but can be much more severe or life-threatening in children and individuals with weak or weakened immune systems. However, current options to treat cryptosporidiosis are limited.

Methods. An in vitro phenotypic screening assay was employed to screen 1200 existing drugs for their anticryptosporidial activity and to determine the inhibitory kinetics of top hits. Selected top hits were further evaluated in mice. The action of the lead compound vorinostat on the parasite histone deacetylase (HDAC) was biochemically validated.

Results. Fifteen compounds exhibited anticryptosporidial activity at nanomolar level in vitro. Among them, the histone deacetylase (HDAC) inhibitor vorinostat retained outstanding efficacy in vitro (half maximal effective concentration, EC_{50} = 203 nM) and in an interleukin 12 knockout mouse model (50% inhibition dose = 7.5 mg/kg). Vorinostat was effective on various parasite developmental stages and could irreversibly kill the parasite. Vorinostat was highly effective against the parasite native HDAC enzymes (half maximal inhibitory concentration, IC_{50} = 90.0 nM) and a recombinant *Cryptosporidium parvum* HDAC (the inhibitor constant, K_i = 123.0 nM).

Conclusions. These findings suggest the potential for repurposing of vorinostat to treat cryptosporidiosis, and imply that the parasite HDAC can be explored for developing more selective anticryptosporidial therapeutics.

Keywords. cryptosporidiosis; vorinostat; histone deacetylase; HDAC; drug repurposing.

Cryptosporidium is a genus of globally distributed protozoan parasites capable of infecting humans and a wide range of vertebrates. Humans are mainly infected by *Cryptosporidium parvum* (zoonotic) and *Cryptosporidium hominis* (human specific), but individuals with weakened immunity such as people with AIDS may also be infected by some other *Cryptosporidium* species (eg, *C. meleagridis*, *C. suis*, *C. canis*, and *C. felis*) [1–3]. These parasites are responsible for numerous water-borne outbreaks and one of the life-threatening opportunistic infections in AIDS patients [4–8]. *Cryptosporidium* is also one of the top 4 diarrhea-causing agents afflicting children in developing countries [9–11]. However, options to treat cryptosporidiosis are highly limited [7]. In fact, nitazoxanide is the single drug approved in the United States for use in immunocompetent individuals, but not in immunocompromised patients. Therefore, there is an urgent need to develop new anticryptosporidial therapeutics.

Screening of known drugs for novel therapeutic activities has the potential for rapid transition from bench to bedside [12–14]. However, high-throughput screening (HTS) of compounds against the growth of the intracellular parasite *C. parvum* in vitro was previously impractical by the labor-intensive traditional assays. Recently, 2 whole-cell phenotypic HTS assays have been developed. The first one is based on high-content imaging analysis (Z′ = 0.21–0.47) that has been used to screen 727 US Food and Drug Administration (FDA)–approved drugs and discovered anticryptosporidial activity of 5-hydroxy-3-methylglutaryl-coenzyme A (HMG-CoA) reductase inhibitors [15]. We have developed the second assay based on quantitative reverse-transcription polymerase chain reaction (qRT-PCR), in which HTS was achieved by directly using cell lysates as the templates to give excellent uniformity and signal-to-noise ratios (ie, >150-fold linear dynamic range in detecting the parasite loads; Z′ = 0.73–0.87) [16].

Using the qRT-PCR–based phenotypic screening assay, we screened the Prestwick Chemical Library containing 1200 known drugs approved by FDA, European Medicines Evaluation Agency, or other agencies to discover potential activities against the growth of *C. parvum* in vitro. Among them, the histone deacetylase (HDAC) inhibitor vorinostat displayed outstanding anticryptosporidial activity in vitro and in vivo. We also

Received 28 September 2017; editorial decision 20 December 2017; accepted 29 December 2017; published online January 2, 2018.

Correspondence: G. Zhu, PhD, Department of Veterinary Pathobiology, College of Veterinary Medicine and Biomedical Sciences, Texas A&M University, College Station, TX 77843-4467 (gzhu@cvm.tamu.edu).

The Journal of Infectious Diseases® 2018;217:1110–7

© The Author(s) 2018. Published by Oxford University Press for the Infectious Diseases Society of America. All rights reserved. For permissions, e-mail: journals.permissions@oup.com.

DOI: 10.1093/infdis/jix689

confirmed that vorinostat could inhibit the activity of native HDACs in the parasite sporozoites and the activity of a recombinant parasite HDAC protein at low nanomolar level. Our data suggest the potential to repurpose vorinostat (and its derivatives) for treating cryptosporidiosis and to explore HDAC as new drug target in the parasite.

METHODS

In Vitro Drug Screening and Drug Efficacy Assays

High-throughput phenotypic screening of existing drugs against the growth of *C. parvum* (Iowa-1 strain) cultured in vitro with HCT-8 cells (ATCC number CCL-244) was performed using our recently developed protocol as described previously [16]. In this assay, *C. parvum* oocysts were used to inoculate the HCT-8 host cell monolayers cultured in 96-well plates, and allowed to undergo excystation and invasion into host cells for 3 hours, followed by the removal of uninvaded parasites by a change of medium containing drugs or diluent and continuous cultivation for 41 hours (total 44 hours infection time). Cell lysates were prepared, diluted, and used directly to evaluate the parasite loads by qRT-PCR in 384-well plates as described [16]. We screened 1200 existing drugs in the Prestwick library at 10 μM in primary screening and 100 top hits at 2 μM in secondary screening, followed by the determination of in vitro anticryptosporidial half maximal effective concentration (EC_{50}) values of selected top hits. In both primary and secondary screening, each plate included 5 wells containing 0.5% dimethyl sulfoxide (DMSO) diluent only as a negative control, and 3 wells containing 140 μM paromomycin (PRM) as a positive control. Selected top hits were used to treat host cells cultured in 96-well plates for 44 hours to evaluate their cytotoxicity using a Cell Titer 96 AQ_{ueous} One Solution Cell Proliferation Assay (MTS assay). Details on the in vitro cultivation protocol, qRT-PCR assay, in vitro cytotoxicity assay, the effect of vorinostat on different parasite developmental stages, effect of pretreatment of host cells with vorinostat on the parasite infection, and drug withdrawal assay are provided in the Supplementary Methods.

Inhibition of the Parasite Native and a Recombinant HDAC Enzyme Activity by Vorinostat

The effect of vorinostat on the activity of the parasite HDACs was examined at both cellular and protein levels. Cell-based assay detected the activity of native HDAC enzymes in the *C. parvum* sporozoites using an HDAC Cell-Based Activity Assay Kit (Cayman Chemical, Ann Arbor, Michigan) that employed a cell-permeable HDAC substrate to evaluate the activity of lysine-specific deacetylases in intact cells. Free sporozoites were prepared by a standard excystation protocol (see Supplementary Methods), suspended in culture medium and aliquoted into a 96-well plate (1.7×10^7 sporozoites/well in 80 μL medium), followed by the addition of 10 μL of vorinostat at various concentrations and 10 μL of HDAC substrate as specified by the manufacturer. After incubation for 2 hours at 37°C, 50 μL of the Lysis/Developer solution was added into each reaction. Plate was briefly shaken on a plate shaker for 1–2 minutes, and then incubated for 15 minutes at 37°C. The viabilities of sporozoites at the beginning and the end of the assay were approximately 84.7% and 72.2% as determined by 4′,6-diamidino-2-phenylindole (DAPI) staining (Supplementary Figure 1). The fluorescent intensities were read on a Fluoroskan Ascent fluorescence plate reader (Thermo Fisher Scientific) (excitation wavelength, λ_{EX} = 355 ± 19.6 nm and emission wavelength, λ_{EM} = 444 ± 6.3 nm).

The effect of vorinostat on a recombinant parasite HDAC protein was evaluated using HDAC Fluorometric Activity Assay Kit (Cayman Chemical). CpHDAC3, an ankyrin repeats-containing, class II-2–like HDAC from *C. parvum* previously characterized by us, was expressed in bacteria as a maltose-binding protein (MBP)-fusion protein and purified into homogeneity as described previously [17]. In this assay, 150 μL per well of reaction solution containing 20 nM CpHDAC3 was aliquoted into a 96-well plate. The reactions started by adding 10 μL of HDAC substrate mixed with vorinostat at various concentrations. After 30 minutes of incubation at 37°C, 40 μL of the developer solution was added into each reaction and then incubated for 15 minutes at room temperature. The fluorescent intensities were read as described above. In both assays, each experimental group included at least 3 biological replicates and 2 technical replicates.

Anticryptosporidial Efficacy of Inhibitors in Mice

The in vivo efficacies of top hits on the cryptosporidial infection were evaluated using an interleukin 12 (IL-12) knockout mouse model as previously described [18]. This model mimics acute cryptosporidial infection, in which the parasite loads would be rapidly intensified with peak oocyst production at around day 7 postinoculation, but the mice would recover by day 14 postinoculation [19]. In this study, 6- to 8-week-old male and female mice were randomly selected and assigned into experimental groups (10 mice/group), and each inoculated with 1000 *C. parvum* oocysts via gavage to start the infection. Mice were then treated with compounds suspended in 5% DMSO in phosphate-buffered saline (PBS) at specified dosage, or vehicle control (5% DMSO in PBS). Paromomycin (2 g/kg/day) was included in selected experiments as positive control.

Treatment was given once daily for 6 days, and mice were euthanized on day 7 (peak infection). Mice were weighed daily from days 0 to 7 postinoculation. Parasite burdens indicated by the production of oocysts in feces were evaluated by flow cytometry as described [20]. In brief, fecal samples were collected from individual mice on day 7 postinoculation, and purified through microscale sucrose gradients in 2.0 mL microcentrifuge tubes. The partially purified stool samples were incubated with an oocyst-specific monoclonal antibody (OW50-FITC) conjugated with fluorescein isothiocyanate for 30 minutes at

37°C as described [20]. Fluorescence-labeled oocysts were then counted on a flow cytometer. The counts were converted to and expressed as oocysts per 100 µL of sample suspension. The mouse studies were approved by the Institutional Animal Care and Use Committees of the Atlanta Veterans Affairs Medical Center (Institutional Animal Care and Use Committee number 2012–020132)

Statistical Analysis

In all in vitro and biochemical assays, at least 3 biological replicates and 2 technical replicates were included for each experimental group. Mann–Whitney *U* test or 1-way analysis of variance, followed by 2-tailed Dunnett or Sidak multiple comparisons tests (depending on whether a dataset contained a single control group for all experimental groups or paired controls for individual experimental groups), were used to assess the statistical significance of the in vitro and in vivo data.

RESULTS

Novel Anticryptosporidial Activity of Existing Drugs In Vitro

We first performed primary screening of 1200 existing drugs at 10 µM. Among them, 1194 drugs displayed varied efficacies, ranging from −128.6% to 99.6% of inhibitions on the parasite growth when assayed at 44 hours postinfection (hpi) (Figure 1; Supplementary Table 1). Eighty-four and 51 drugs inhibited the parasite growth by >80% and >90%, respectively. Anticryptosporidial efficacy could not be determined for 6 drugs due to high cytotoxicity to host cells (ie, >90% reduction of 18S ribosomal RNA levels in host cells). Among the 1194 drugs, 20 also showed certain levels of cytotoxicity (ie, 50%–90% inhibition on host cells by qRT-PCR) (Supplementary Table 1).

In secondary screening, we tested the top 100 compounds at 2.0 µM, in which 15 compounds retained >70% anticryptosporidial efficacy (Supplementary Table 2). Subsequent dose-response experiments revealed that all 15 compounds had in vitro anticryptosporidial EC_{50} values between 0.044 µM and approximately 1.0 µM (Table 1). Compounds showing low-nanomolar-level activities included monensin (EC_{50} = 44 nM), docetaxel (87 nM), paclitaxel (99 nM), podophyllotoxin (138 nM), colchicine (187 nM), and vorinostat (203 nM) (Table 1).

Notably, 10 of the 15 compounds were inhibitors of microtubule assembly/disassembly (n = 6; including docetaxel, paclitaxel, podophyllotoxin, colchicine, albendazole, and mebendazole) and DNA metabolism (n = 4; including vorinostat, trifluridine, daunorubicin, and doxorubicin) that are classified as antineoplastic drugs (n = 8) or anthelmintics (n = 2) (Table 1). These observations indicate that microtubule and DNA metabolism in the parasite may be highly exploitable as drug targets. The remaining 5 compounds target various other pathways, including membrane potential, protein folding, protein kinase, H1 receptor, and sulfhydryl molecules. These top hits displayed satisfactory to outstanding in vitro safety interval (SI) based on the ratios between the concentrations for half maximal inhibition of cell proliferation (TC_{50} values) on HCT-8 cells and anticryptosporidial EC_{50} values (ie, SI = TC_{50} / EC_{50}; $N_{[SI>100]}$ = 6 and $N_{[SI=9.5–100]}$ = 9) (Table 1).

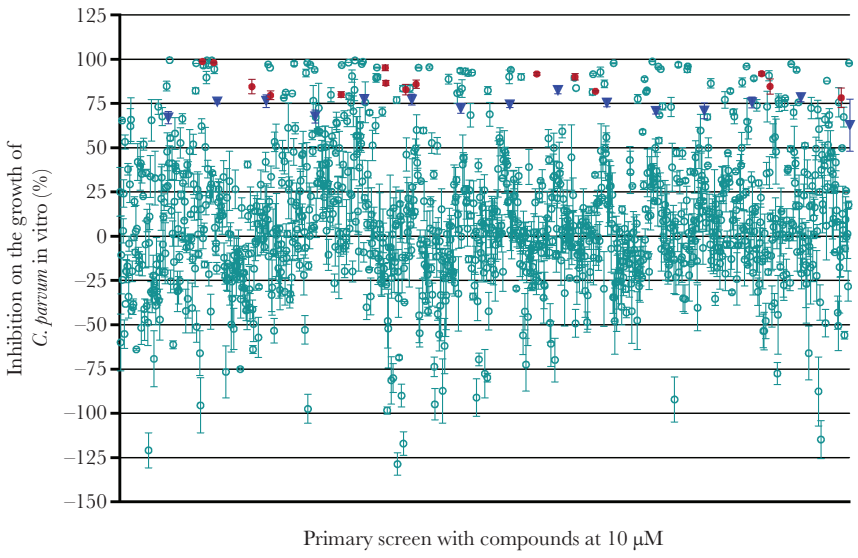

Figure 1. High-throughput screening of 1200 existing drugs. Scatterplot showing the percent inhibition of the growth of *Cryptosporidium parvum* in vitro by 1994 drugs at 10 µM (green and red circles). Six drugs were not included in the plot due to high cytotoxicity. The red circles indicate the 15 top hits retaining excellent efficacy at 2 µM in secondary screening and selected for determining their antiparasitic half maximal effective concentration (EC_{50}) values (also see Table 1). The blue triangles indicate the paromomycin-positive controls (140 µM, 3 wells/plate). Each plate included 0.5% dimethyl sulfoxide diluent only as negative control (5 wells/plate). Bars show the standard error of the mean (n ≥ 3).

Table 1. Efficacy of 15 Top Hits Against the Growth of *Cryptosporidium parvum* In Vitro Determined by Quantitative Reverse-Transcription Polymerase Chain Reaction Assay, Their Cytotoxicity on HCT-8 Cells Determined by a MTS Cell Proliferation Assay, and Safety Intervals

Compound	CAS No.	Description	Target Group	EC_{50}, μM	TC_{50}, μM	Safety Interval
Monensin	22373-78-0	Anticoccidial; monovalent cation ionophore	Membrane potential	0.044	>100	>2000
Docetaxel	114977-28-5	Antineoplastic; microtubule dissassembly inhibitor	Cytoskeleton	0.087	54.17	623
Paclitaxel	**33069-62-4**	**Antineoplastic; microtubule dissassembly inhibitor**	**Cytoskeleton**	**0.099**	**30.25**	**306**
Podophyllotoxin	518-28-5	Antineoplastic; microtubule assembly inhibitor (medical cream)	Cytoskeleton	0.138	10.33	75
Colchicine	64-86-8	Antineoplastic; microtubule assembly inhibitor	Cytoskeleton	0.187	42.83	229
Vorinostat	**149647-78-9**	**Antineoplastic; HDAC inhibitor**	**DNA metabolism**	**0.203**	**2.32**	**11.4**
Thimerosal	54-64-8	Antiseptic/antifungal; organomercury compound	Sulfhydryl molecules	0.501	28.39	62.1
Vatalanib	**97-59-6**	**Antineoplastic; protein kinase inhibitor**	**Protein kinase**	**0.322**	**33.7**	**105**
Trifluridine	70-00-8	Antiviral; nucleic acid synthesis inhibitor	DNA metabolism	0.543	>100	>184
Astemizole	68844-77-9	Antihistamine; H1 receptor antagonist	Receptor	0.717	10.86	15.4
Albendazole	54965-21-8	Anthelmintics; microtubule assembly inhibitor	Cytoskeleton	0.756	>100	>132.3
Daunorubicin	23541-50-6	Antineoplastic; DNA intercalant (poison)	DNA metabolism	0.787	7.46	9.5
Mebendazole	31431-39-7	Anthelmintics; microtubule assembly inhibitor	Cytoskeleton	0.95	58.76	61.9
Cyclosporin A	59865-13-3	Immunosuppressant; cyclophilin-binding, IL-2 synthesis inhibitor	Protein folding	1.031	18.52	18
Doxorubicin	25316-40-9	Antineoplastic; DNA intercalant, DNA topoisomerase II inhibitor	DNA metabolism	1.092	12.11	11.1

Bold fonts indicate compounds evaluated for their anticryptosporidial activity in mice (also see Table 2).

Abbreviations: CAS, Chemical Abstracts Service; EC_{50}, half maximal effective concentration; HDAC, histone deacetylase; IL-2, interleukin 2; MTS, 3-(4,5-dimethylthiazol-2-yl)-5-(3-carboxymethoxyphenyl)-2-(4-sulfophenyl)-2H-tetrazolium, inner salt; TC_{50}, concentration for half maximal inhibition of cell proliferation determined by MTS assay.

In Vivo Activity of Vorinostat Against Cryptosporidiosis

Based on drug medical indications, we first selected 3 top hits representing several classes of inhibitors and evaluated their anticryptosporidial efficacy in vivo at a single dose comparable to those used in humans based on body surface area conversion between humans and mice [21]. Auranofin was also included in the study for convenience, because it is not only a repurposing candidate drug against *Entamoeba histolytica* [22], but also efficacious against *Cryptosporidium* in vitro [23]. This study also confirmed the in vitro efficacy of auranofin, although it was not one of the top 15 drugs (ie, EC_{50} = 1.8 μM, TC_{50} = 3.2 μM, and SI = 1.8). Paromomycin was used as a positive control. By treating mice infected with *C. parvum* for 6 days at a single daily oral dose, vorinostat (25.0 mg/kg) and paclitaxel (2.0 mg/kg) displayed the most satisfactory efficacy against acute cryptosporidial infection in IL-12 knockout mice (ie, up to 91.1% and 78.6% reduction, respectively, of oocyst production in mice) (Table 2). Vatalanib (25.0 mg/kg) showed moderate efficacy

Table 2. Efficacies of Selected Top Hits on the Acute Infection of *Cryptosporidium parvum* in Interleukin 12 Knockout Mice

Compound	Dose, mg/kg/d	No.	Inhibition on Production of *C. parvum* Oocysts[a]		Weight Gain in Drug Testing (7 dpi)	Weight Gain in Toxicity Assay (4 dpi)
			5 dpi	7 dpi		
Vorinostat	25.0	10	77.9%****	91.1%***	–0.20%	3.30%
Paclitaxel	2.0	10	50.8%	78.6%**	0.15%	–0.40%
Vatalanib	25.0	10	19.4%	51.9%	0.18%	–4.30%
Auranofin	6.0	11	–95.1%*	6.7%	0.05%	Not tested
Paromomycin	2000	5	45.4%	82.6%**	0.86%	Not tested
Vehicle control	5% DMSO	10	0%	0%	0.39%	–2.20%

Abbreviations: DMSO, dimethyl sulfoxide; dpi, days postinoculation.

[a]Oocyst production was counted on days 5 and 7 postinoculation (dpi).

*P < .05, **P < .01, *** P < .001, **** P < .0001 (2-tailed Mann–Whitney U test, vs untreated vehicle control).

(up to 51.9% reduction), whereas auranofin did not display any anticryptosporidial activity in vivo (up to 6.7% reduction). The positive control paromomycin produced efficacy at a level similar to previous reported studies (82.6% reduction at 2000 mg/kg) (Table 2) [18, 24].

As both vorinostat (aka suberanilohydroxamic acid [SAHA], brand name Zolina) and paclitaxel (brand name Taxol) are antineoplastic drugs, we then carried out more detailed studies on the vorinostat that showed the highest anticryptosporidial efficacy in mice. We first validated the dose-dependent activity in mice, in which vorinostat at 10, 25, 50, and 100 mg/kg (single daily dose for 6 days) reduced the production of parasite oocysts by 62.0% (±30.3), 88.8% (±14.9), 94.3% (±4.2), and 99.0% (±0.5), respectively (Figure 2). The estimated in vivo 50% inhibition dose (ID_{50}) value was approximately 7.5 mg/kg. The efficacious doses of vorinostat in mice (10–100 mg/kg/day) are equivalent to 48.5–484.8 mg per 60-kg adult based on body surface area conversion [21], suggesting that the dosage currently recommended for use in patients (ie, 400 mg/day oral dose for adults) may potentially be applicable to treating human cryptosporidiosis.

Irreversible Killing of *C. parvum* by Vorinostat

More detailed in vitro studies also showed that vorinostat was highly effective against various developmental stages of *C. parvum* in vitro (Figure 3A and 3B). More specifically, vorinostat at 400 nM (a dose giving approximately 80%–90% inhibition in vitro) was effective against the invasion of sporozoites (28% reduction in the group receiving treatment from 0–3 hpi) and the growth of early trophozoites (34.8% reduction in 0–6 hpi treatment group) (ie, the 0–3 hpi and 0–6 hpi groups in Figure 3A). Vorinostat reduced the first 20 hours parasite growth by 72.0% (3–20 hpi treatment group in Figure 3A). At the 20 hpi time point, the parasites developed into a mixed population of trophozoites with single nucleus, and early to late stages of meronts with 2–8 nuclei (Supplementary Figure 2). In the positive control group (ie, 3–44 hpi treatment group in Figure 3A), vorinostat reduced the parasite growth by 88.7% reduction as expected. At the 44 hpi time point, the parasites developed into a mixed population of trophozoites, various stages of meronts, and early sexual stages (Supplementary Figure 2).

In a drug withdrawal assay (Figure 3B), the growth of *C. parvum* in vitro was inhibited by 92.3% when the parasites were treated with vorinostat from 3–20 hpi and allowed to recover for 24 hours after the removal of drug, and by 72.1% when treated only from 20 to 44 hpi. These observations indicated that vorinostat could act on various parasite developmental stages, and the inhibition of parasite growth by this compound was likely irreversible.

The anticryptosporidial activity was unlikely attributed to the effect of vorinostat on host cells, because vorinostat was highly efficacious at concentrations nontoxic to host cells (ie, EC_{50} = 203 nM vs TC_{50} = 2320 nM) (Table 1). Additionally, pretreatment of host cells with a high dose of vorinostat (ie, 400 nM) for 22 hours had no effect on the parasite invasion and early trophozoite development (Figure 3C).

Nanomolar Inhibitory Activity of Vorinostat on the Parasite HDACs

To further validate the inhibition mechanism of vorinostat on the parasite, we tested the activity of vorinostat against the native HDAC enzymes present in live *C. parvum* sporozoites—the only stage for which pure parasite materials could be practically

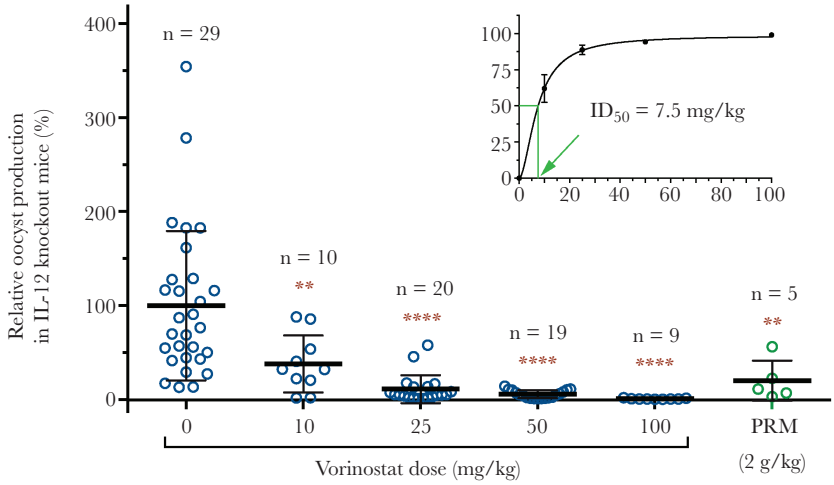

Figure 2. Efficacy of vorinostat on the production of *Cryptosporidium parvum* oocysts in a mouse model of acute cryptosporidiosis. Interleukin 12 (IL-12) knockout mice were infected with *C. parvum* and received treatment of vorinostat at specified single daily oral doses for 6 days. Vehicle only (5% dimethyl sulfoxide in phosphate-buffered saline) was set as negative control and paromomycin (PRM) at 2 g/kg single daily dose was included as a positive control. Oocyst production was measured on the seventh day postinfection. Inset shows a dose-dependent curve of data derived from the same study for estimating 50% inhibition dose (ID_{50}). Bars show the standard error of the mean from the specified number of samples (n). Asterisks indicate levels of statistical significance between individual groups and the control receiving no drug by Dunnett multiple comparison test. $^{**}P < .01$, $^{****}P < .0001$.

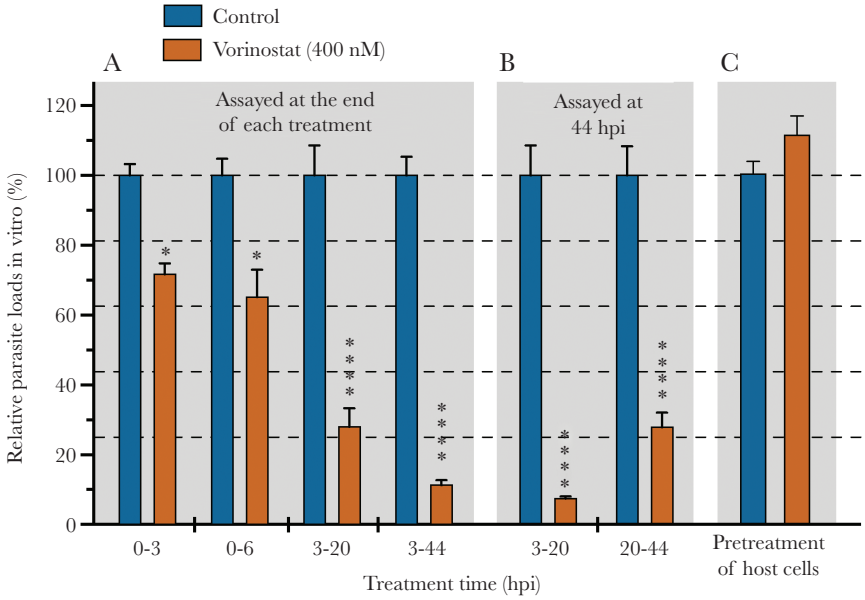

Figure 3. Effect of vorinostat (400 nM) on various developmental stages of *Cryptosporidium parvum* in vitro. *A*, Effect of vorinostat on the invasion of *C. parvum* in vitro (0–3 hours postinfection [hpi] group), the invasion and early-stage development of invaded sporozoites into trophozoites, each containing a single nucleus (0–6 hpi), the first 20 h development forming trophozoites and meronts containing ≥2 nuclei (3–20 hpi), and the later development of forming a mixed population of trophozoites, meronts, and early sexual stages of parasites (20–44 hpi) (also see Supplementary Figure 2 for the morphology of intracellular parasites at the specified time points). In this assay, HCT-8 cells were inoculated with *C. parvum* oocysts for 3 h (or 6 h in the 0–6 hpi group), followed by the removal of intact oocysts and uninfected sporozoites and continuous cultivation as specified. The parasite loads were determined at the end of each treatment. *B*, In vitro drug withdrawal assay, in which vorinostat (400 nM) was added into the cultivation after the invasion and removal of free parasite at 3 hpi time, followed by drug washout at 20 hpi (3–20 hpi group) and continuous cultivation without drug for up to 44 hpi. Samples receiving a full course of treatment (3–44 hpi group) were included for comparison. The parasite loads were assayed at 44 hpi. *C*, Effect of pretreatment of host cell on the parasite invasion and early stage of development, in which HCT-8 cells were treated with vorinostat (400 nM) for 20 h, followed by drug washout and inoculation of excysted *C. parvum* sporozoites for 3 h in the absence of vorinostat. Bars show the standard error of the mean from the specified number of samples (n ≥ 6). Asterisks indicate levels of statistical significance between individual groups and corresponding controls receiving no drug by Sidak multiple comparisons test. **P* < .05, *****P* < .0001.

obtained, and against a recombinant CpHDAC3 representing 1 of the 5 HDAC/sir2 family proteins in the parasite previously characterized by us [17]. We observed outstanding low nanomolar inhibitory activity in both assays (ie, half maximal inhibitory concentration [IC_{50}] = 90.0 nM on native HDAC activity in the sporozoites (Figure 4A; IC_{50} = 399.0 nM and the inhibition constant [K_i] = 123.0 nM on recombinant CpHDAC3 enzyme activity Figure 4B). These observations support the hypothesis that vorinostat inhibits *C. parvum* growth by acting on the parasite HDAC enzymes.

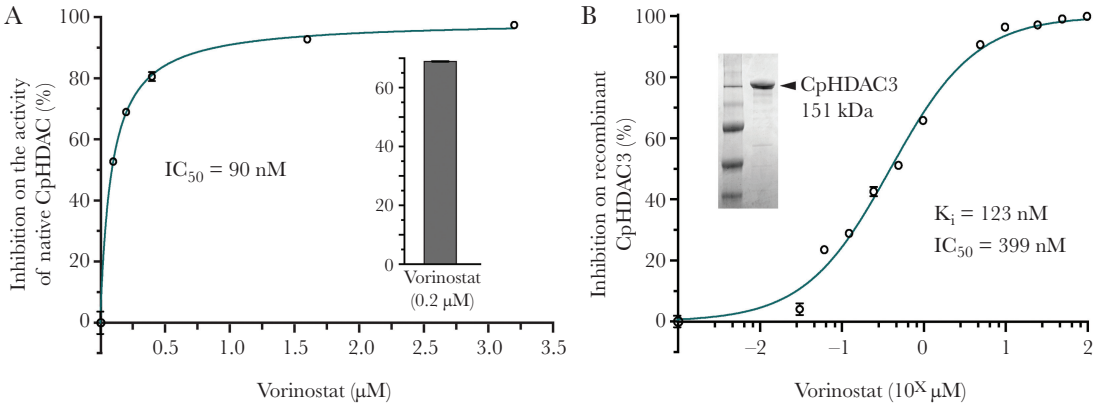

Figure 4. Dose-dependent inhibition of *Cryptosporidium parvum* histone deacetylase (CpHDAC) activity by vorinostat. *A*, Inhibition of native histone deacetylase (HDAC) activity present in live *C. parvum* sporozoites by vorinostat as determined using a cell-based HDAC activity assay. Inset shows the single-dose data obtained during the assay optimization. *B*, Inhibition of the enzymatic activity of recombinant CpHDAC3 protein by vorinostat. Inset shows an sodium dodecyl sulfate–polyacrylamide gel electrophoresis image of purified recombinant, maltose-binding protein–fusion CpHDAC3 protein. Bars show the standard error of the mean (n ≥ 3). 10^X in (***B***) represents the power of 10 (ie, the X-axis in logarithm scale). Abbreviations: CpHDAC, *Cryptosporidium parvum* histone deacetylase; IC_{50}, half maximal inhibition concentration; K_i, the inhibition constant.

DISCUSSION

Currently, no drug is FDA approved to treat cryptosporidiosis in immunocompromised patients, although a single drug (ie, nitazoxanide) has been approved in the United States for use in immunocompetent patients [25, 26]. Even so, nitazoxanide is not fully effective, and its mechanism of action is ill-defined. Therefore, an urgent need exists for the development of new anticryptosporidial drugs, particularly for treating AIDS patients and children.

Anticryptosporidial drug development has been significantly hindered by the unusual metabolic features in this parasite. Many well-defined and promising drug targets found in other apicomplexans are either absent or highly divergent in *Cryptosporidium* [7, 27]. However, recent studies have led to the discovery of several promising leads with known targets in the parasite, including compound 1294 on calcium-dependent protein kinases [28], P131 on inosine-5′-monophosphate dehydrogenase [29], triacsin C on fatty acyl-CoA synthetase [18], and more recently, KDU731 on phosphatidylinositol-4-OH kinase [30]. Nonetheless, all these hits/leads are in the preclinical phase of investigation. Even if 1 or more leads are successfully developed into therapeutics, anticryptosporidial drugs with different targets will add to the diversified pool of available drugs.

The present study aimed to identify novel anticryptosporidial activities from existing drugs for potential repurposing. We have discovered that vorinostat and a few other drugs such as paclitaxel displayed outstanding efficacy against cryptosporidial infection both in vitro and in vivo. Vorinostat is a well-characterized HDAC inhibitor [31]. It has been FDA-approved to treat cutaneous T-cell lymphoma and under clinical trials for treating several other types of cancers. Additionally, vorinostat was also shown effects against latently human immunodeficiency virus (HIV)–infected T cells and under clinical trials to treat HIV infection [32, 33], suggesting an exciting potential to develop vorinostat for treating both HIV and the AIDS-related opportunistic infection cryptosporidiosis.

Collectively, we have discovered outstanding in vitro and in vivo anticryptosporidial activity of the FDA-approved drug vorinostat. We also showed that low nanomolar level of vorinostat can efficiently inhibit *C. parvum* HDAC activity and could irreversibly kill the parasite. These discoveries offer a promising opportunity for repurposing vorinostat to treat cryptosporidiosis, for evaluating its existing analogues, and for exploring HDAC as a new target for developing more efficacious and selective anticryptosporidial therapeutics.

Supplementary Data

Supplementary materials are available at *The Journal of Infectious Diseases* online. Consisting of data provided by the authors to benefit the reader, the posted materials are not copyedited and are the sole responsibility of the authors, so questions or comments should be addressed to the corresponding author.

Notes

Author contributions. G. Z., F. G., and H. Z. designed the HTS screening studies and in vitro efficacy assays. H. Z. and F. G. performed HTS and in vitro efficacy assays. J. R. M. and G. Z. designed the in vivo experiments. J. R. M. and N. N. M. performed in vivo experiments. F. G. and H. Z. designed and performed the HDAC inhibition assay. G. Z., H. Z., F. G., and J. R. M. wrote the manuscript.

Financial support. This work was supported by the National Institute of Allergy and Infectious Diseases at the National Institutes of Health (grant number R21 AI099850 to G. Z.) and by the Atlanta Veterans Affairs Medical Center (VA Merit program to J. M.).

Potential conflicts of interest. All authors: No reported conflicts of interest. All authors have submitted the ICMJE Form for Disclosure of Potential Conflicts of Interest. Conflicts that the editors consider relevant to the content of the manuscript have been disclosed.

References

1. Tzipori S, Widmer G. The biology of *Cryptosporidium*. Contrib Microbiol **2000**; 6:1–32.
2. Chen XM, Keithly JS, Paya CV, LaRusso NF. Cryptosporidiosis. N Engl J Med **2002**; 346:1723–31.
3. Leav BA, Mackay M, Ward HD. *Cryptosporidium* species: new insights and old challenges. Clin Infect Dis **2003**; 36:903–8.
4. DuPont HL. Persistent diarrhea: a clinical review. JAMA **2016**; 315:2712–23.
5. Cacciò SM, Chalmers RM. Human cryptosporidiosis in Europe. Clin Microbiol Infect **2016**; 22:471–80.
6. Turkeltaub JA, McCarty TR 3rd, Hotez PJ. The intestinal protozoa: emerging impact on global health and development. Curr Opin Gastroenterol **2015**; 31:38–44.
7. Checkley W, White AC Jr, Jaganath D, et al. A review of the global burden, novel diagnostics, therapeutics, and vaccine targets for *Cryptosporidium*. Lancet Infect Dis **2015**; 15:85–94.
8. O'connor RM, Shaffie R, Kang G, Ward HD. Cryptosporidiosis in patients with HIV/AIDS. AIDS **2011**; 25:549–60.
9. Kotloff KL, Nataro JP, Blackwelder WC, et al. Burden and aetiology of diarrhoeal disease in infants and young children in developing countries (the Global Enteric Multicenter Study, GEMS): a prospective, case-control study. Lancet **2013**; 382:209–22.
10. Sow SO, Muhsen K, Nasrin D, et al. The burden of *Cryptosporidium* diarrheal disease among children < 24 months of age in moderate/high mortality regions of sub-Saharan Africa and South Asia, utilizing data from the Global Enteric Multicenter Study (GEMS). PLoS Negl Trop Dis **2016**; 10:e0004729.

11. Liu J, Platts-Mills JA, Juma J, et al. Use of quantitative molecular diagnostic methods to identify causes of diarrhoea in children: a reanalysis of the GEMS case-control study. Lancet **2016**; 388:1291–301.
12. Savoia D. New antimicrobial approaches: reuse of old drugs. Curr Drug Targets **2016**; 17:731–8.
13. Padhy BM, Gupta YK. Drug repositioning: re-investigating existing drugs for new therapeutic indications. J Postgrad Med **2011**; 57:153–60.
14. Ashburn TT, Thor KB. Drug repositioning: identifying and developing new uses for existing drugs. Nat Rev Drug Discov **2004**; 3:673–83.
15. Bessoff K, Sateriale A, Lee KK, Huston CD. Drug repurposing screen reveals FDA-approved inhibitors of human HMG-CoA reductase and isoprenoid synthesis that block *Cryptosporidium parvum* growth. Antimicrob Agents Chemother **2013**; 57:1804–14.
16. Zhang H, Zhu G. Quantitative RT-PCR assay for high-throughput screening (HTS) of drugs against the growth of *Cryptosporidium parvum* in vitro. Front Microbiol **2015**; 6:991.
17. Rider SD Jr, Zhu G. An apicomplexan ankyrin-repeat histone deacetylase with relatives in photosynthetic eukaryotes. Int J Parasitol **2009**; 39:747–54.
18. Guo F, Zhang H, Fritzler JM, et al. Amelioration of *Cryptosporidium parvum* infection in vitro and in vivo by targeting parasite fatty acyl-coenzyme A synthetases. J Infect Dis **2014**; 209:1279–87.
19. Campbell LD, Stewart JN, Mead JR. Susceptibility to *Cryptosporidium parvum* infections in cytokine- and chemokine-receptor knockout mice. J Parasitol **2002**; 88:1014–6.
20. Arrowood MJ, Hurd MR, Mead JR. A new method for evaluating experimental cryptosporidial parasite loads using immunofluorescent flow cytometry. J Parasitol **1995**; 81:404–9.
21. Reagan-Shaw S, Nihal M, Ahmad N. Dose translation from animal to human studies revisited. FASEB J **2008**; 22:659–61.
22. Debnath A, Parsonage D, Andrade RM, et al. A high-throughput drug screen for *Entamoeba histolytica* identifies a new lead and target. Nat Med **2012**; 18:956–60.
23. Debnath A, Ndao M, Reed SL. Reprofiled drug targets ancient protozoans: drug discovery for parasitic diarrheal diseases. Gut Microbes **2013**; 4:66–71.
24. Healey MC, Yang S, Rasmussen KR, Jackson MK, Du C. Therapeutic efficacy of paromomycin in immunosuppressed adult mice infected with *Cryptosporidium parvum*. J Parasitol **1995**; 81:114–6.
25. Fox LM, Saravolatz LD. Nitazoxanide: a new thiazolide antiparasitic agent. Clin Infect Dis **2005**; 40:1173–80.
26. White AC Jr. Nitazoxanide: an important advance in anti-parasitic therapy. Am J Trop Med Hyg **2003**; 68:382–3.
27. Rider SD Jr, Zhu G. *Cryptosporidium*: genomic and biochemical features. Exp Parasitol **2010**; 124:2–9.
28. Castellanos-Gonzalez A, White AC Jr, Ojo KK, et al. A novel calcium-dependent protein kinase inhibitor as a lead compound for treating cryptosporidiosis. J Infect Dis **2013**; 208:1342–8.
29. Gorla SK, McNair NN, Yang G, et al. Validation of IMP dehydrogenase inhibitors in a mouse model of cryptosporidiosis. Antimicrob Agents Chemother **2014**; 58:1603–14.
30. Manjunatha UH, Vinayak S, Zambriski JA, et al. A *Cryptosporidium* PI(4)K inhibitor is a drug candidate for cryptosporidiosis. Nature **2017**; 546:376–80.
31. Marks PA, Breslow R. Dimethyl sulfoxide to vorinostat: development of this histone deacetylase inhibitor as an anticancer drug. Nat Biotechnol **2007**; 25:84–90.
32. Ke R, Lewin SR, Elliott JH, Perelson AS. Modeling the effects of vorinostat in vivo reveals both transient and delayed HIV transcriptional activation and minimal killing of latently infected cells. PLoS Pathog **2015**; 11:e1005237.
33. Elliott JH, Wightman F, Solomon A, et al. Activation of HIV transcription with short-course vorinostat in HIV-infected patients on suppressive antiretroviral therapy. PLoS Pathog **2014**; 10:e1004473.